CORE
Metadata, citation and similar papers at core.ac.uk
Provided by University of Central Florida (UCF): STARS (Showcase of Text, Archives, Research & Scholarship)

University of Central Florida
STARS

Faculty Bibliography 2000s
Faculty Bibliography

1-1-2008

Coupled dipole method for modeling optical properties of large-scale random media

S. Sukhov
University of Central Florida

D. Haefner
University of Central Florida

A. Dogariu
University of Central Florida

Find similar works at: https://stars.library.ucf.edu/facultybib2000
University of Central Florida Libraries http://library.ucf.edu

This Article is brought to you for free and open access by the Faculty Bibliography at STARS. It has been accepted for inclusion in Faculty Bibliography 2000s by an authorized administrator of STARS. For more information, please contact STARS@ucf.edu.

Recommended Citation

Sukhov, S.; Haefner, D.; and Dogariu, A., "Coupled dipole method for modeling optical properties of large-scale random media" (2008). *Faculty Bibliography 2000s*. 1025.
https://stars.library.ucf.edu/facultybib2000/1025

Coupled dipole method for modeling optical properties of large-scale random media

S. Sukhov, D. Haefner, and A. Dogariu
CREOL, College of Optics and Photonics, University of Central Florida, Orlando, Florida 32816-2700, USA
(Received 3 December 2007; published 23 June 2008)

We present an extension of the coupled dipole approximation technique to model optical properties of large-scale slabs of homogeneous and inhomogeneous materials. This method is based on a modification of the Green's function to take into account the interaction between dipoles located at arbitrary distances within the slab. This method allows modeling of various aspects of the structural morphology of composite materials, including component size and spatial distribution as well as surface roughness effects. Our procedure provides an adequate description of far-field optical properties such as the specular and diffuse reflection of light.

DOI: 10.1103/PhysRevE.77.066709 PACS number(s): 02.70.−c, 42.25.Dd, 78.20.Bh

I. INTRODUCTION

Understanding the optical properties of random media is essential for applications in colloidal, material, and biological sciences. These properties are in many instances determined by complex phenomena such as multiple light scattering. The analytical description of light interaction with such materials is very complicated, and usually requires simplifying approaches like the effective medium approximation (for sparse distribution of inhomogeneities smaller than the wavelength), quasicrystalline approximation, radiative transfer theory, some heuristic approximations based on this theory such as the Monte Carlo technique [1], or phenomenological theories such as the microphysical treatment of coherent backscattering or strong localization [2–7].

Along with such approximate approaches, one can also attempt to solve boundary value problems of light interaction with random media by applying direct numerical techniques based on Maxwell's equations, such as the pseudospectral time-domain technique [8]. In the case of random media, additional requirements are imposed by the statistical nature of the light-matter interaction. For instance, in Ref. [9], the *T*-matrix method was used to study multiple scattering effects in discrete random media with a size parameter $kR=40$, filled with inclusions with size parameters $kr=4$, where k is the wave number in the surrounding medium, and R and r represent the sizes of the scattering object and inclusions, respectively. In Ref. [10], the *T*-matrix method was used to consider scattering of a Gaussian beam from a thin layer of randomly distributed spherical particles. Other available numerical techniques to describe light interaction with random media include the finite-difference time-domain (FDTD) method, finite-element method (FEM), coupled dipole approximation (CDA), etc. Of these numerical tools, the CDA may be the preferred technique because it does not suffer from some of the important disadvantages of the other alternatives, such as the need to discretize the space outside the region of interaction, or to implement suitable boundary conditions to prevent nonphysical reflections from the boundaries of the computational domain. Another advantage of the CDA is that it can be easily applied to any inclusion shape, which can be inhomogeneous or anisotropic.

In its original form, the CDA was developed to study optical properties of small scattering objects [11,12]. Later, this method was extended to describe scattering from objects on a surface [13,14], or the wave interaction with layered media [15]. A notable recent extension of the CDA method is its use for characterizing the optical responses of periodic structures [16] and the scattering from defects in periodic structures [17]. In Ref. [18], the CDA was used to model light scattering from coatings. The coating layer was modeled either as cylindrical slabs or as large spheres with spherical pigments packed inside. The size parameter of the modeled cylinders was limited to $kR\approx 45$, and that of spheres to $kR=11.3$. Thus, in the traditional formulation, the CDA can describe scattering from inhomogeneous objects with relatively small dimensions. In this paper we present an extension of the coupled dipole approximation to describe reflection and scattering of light by large-scale random media, namely, by inhomogeneous dielectric slabs.

II. THE COUPLED DIPOLE APPROXIMATION

The coupled dipole approximation is a numerical technique that discretizes a continuum volume into a finite array of polarizable point dipoles [11,12]. These dipoles react to both the local field, and, by the use of the dyadic Green's function, to the field generated by its interactions with all other dipoles on the lattice. The dyadic Green's function accounts for the complete interaction due to the interdipole separation including both the near- and far-field components. The dielectric material properties are related to the modeled structure through the local polarizability (self-term of interaction) at each dipole.

The field at each of the dipoles can be written as the summation of both the incident field and the contributions occurring from the interaction with all the other dipoles on the lattice [11],

$$\mathbf{E}(\mathbf{r}_j) = \mathbf{E}^{\mathrm{inc}}(\mathbf{r}_j) + \sum_{\substack{k=1 \\ k\neq j}}^{N} \mathbf{E}_k^{\mathrm{dip}}(\mathbf{r}_j), \tag{1}$$

where $\mathbf{E}_k^{\mathrm{dip}}(\mathbf{r}_j)$ is the electric field radiated to the point $\mathbf{r}_j$ by the kth dipole $\mathbf{P}_k$. Considering a dipole at an arbitrary location $\mathbf{r}_k$, the radiated field can be written as

 ©2008 The American Physical Society

$$\mathbf{E}_k^{\mathrm{dip}}(\mathbf{r}_j) = [A(\mathbf{r}_j, \mathbf{r}_k)]\mathbf{P}_k, \tag{2}$$

where the dipole moment $\mathbf{P}_k$ is related to the field $\mathbf{E}(\mathbf{r}_k)$ through the polarizability α_k: $\mathbf{P}_k = \alpha_k \mathbf{E}(\mathbf{r}_k)$. In the general case α_k is a tensor [19]. $A(\mathbf{r}_j, \mathbf{r}_k)$ accounts for the interaction matrix; this matrix is dense and symmetric, of size $3N \times 3N$, where N is the total number of dipoles used. The explicit expression for $A(\mathbf{r}_j, \mathbf{r}_k)$ in the conventional form of the CDA is the following [11,12]:

$$A(\mathbf{r}_j, \mathbf{r}_k) = \frac{\exp(ikr_{jk})}{r_{jk}} \left(-k^2(\hat{\mathbf{r}}_{jk} \otimes \hat{\mathbf{r}}_{jk} - I_3) + \frac{1 - ikr_{jk}}{r_{jk}^2} \times (3\hat{\mathbf{r}}_{jk} \otimes \hat{\mathbf{r}}_{jk} - I_3) \right), \tag{3}$$

where $r_{jk} \equiv |\mathbf{r}_j - \mathbf{r}_k|$ and $\hat{\mathbf{r}}_{jk} \equiv (\mathbf{r}_j - \mathbf{r}_k)/r_{jk}$, $k = \omega/c$ is the wave number in vacuum, the symbol $\otimes$ denotes the outer product of vectors, and I_3 is the 3×3 identity matrix.

The common procedure of field calculation in the CDA is based on the solution of the system of equations (1) with respect to $\mathbf{E}(\mathbf{r}_j)$. The solution of Eq. (1) gives the electric field strength at every point of our discretized medium. When this field is known, the field at any arbitrary point may be easily calculated from Eq. (1) by replacing $\mathbf{r}_j \to \mathbf{r}$.

To accurately describe scattering from an object with dimensions comparable to the wavelength, one has to operate with very large matrices; consequently, direct methods for solving the system of equations (1) are not applicable. The main challenge of the CDA numerical approach is that of solving the large system of linear equations using nonstationary iterative methods such as conjugate gradient, biconjugate gradient stabilized, quasiminimal residual techniques, etc. [20]. As in all nonstationary approaches, the accuracy and the rate of convergence can depend very heavily on the preconditioner used to approximate the inverse of Eq. (3) [21].

If the point dipoles are arranged on a cubic lattice throughout the modeling volume, a dramatic decrease in memory requirements and computational time can be accomplished through the use of Fourier transforms [22]. The system of equations outlined in (1) can be transposed into a convolution, taking into account the symmetry properties of the $A(\mathbf{r}_j, \mathbf{r}_k)$ matrix and storing only unique vector interactions.

III. RANDOM MATERIALS AND THE CDA

Along with describing the scattering from homogeneous objects, the CDA may also be used to characterize the optical properties of inhomogeneous (random) materials [18,23,24]. When modeling a random composite material, dipoles with different polarizabilities are randomly distributed across the lattice in proportions determined by the medium's composition. The value of the polarizability for every dipole is determined by the local dielectric properties of the inhomogeneous medium. One advantage of the CDA in the modeling of random media is its ability to easily describe interaction and multiple scattering between inclusions of arbitrary size and shape. Numerically, each spherical inclusion is modeled by one or more dipoles depending on the inclusion size. Figure 1 shows an example of spheres randomly distributed throughout the cubic lattice. This random distribution of polarizabilities constitutes one realization of the randomly inhomogeneous medium. To adequately describe the measurable properties of inhomogeneous media, usually it is necessary to calculate the scattered fields for many such realizations. For each realization of the sample, the far-field coherent superposition of the dipolar contributions is recorded. After a large number of these realizations, an intensity distribution is created and the statistically relevant information such as the average scattered intensity in a specified direction, optical contrast, etc. can be analyzed [23]. It is important to point out that, in the case of inhomogeneous materials, the number of iterations needed to approach the solution of Eq. (1) usually depends on the refractive index contrast between the different constituents, the volume fraction of inclusions, and also on the initial estimate, interdipole spacing, and dimensions of the modeled medium.

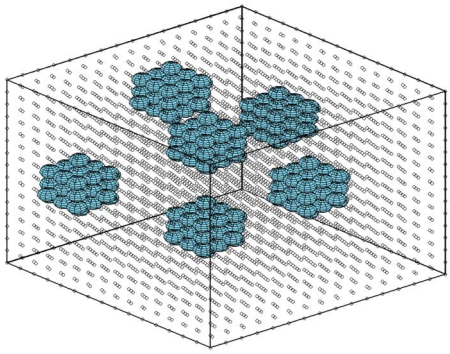

FIG. 1. (Color online) One realization of a random medium: inclusions (dark) are randomly distributed throughout the lattice (dipoles of the host material are shown as small circles) according to the prescribed volume fraction. The modeling cube consists of $16 \times 16 \times 16$ dipoles. The figure corresponds to a 5% concentration of inclusions, and each inclusion consists of 33 dipoles.

IV. EXTENSION TO INFINITE SLABS

One of the challenges of implementing coupled dipole algorithms is the rapid increase of memory requirements for large numbers of dipoles. Thus, the CDA method described above can be used for describing scattering only from limited size objects. For instance, for a refractive index $n=2$, the manageable dimensions cannot exceed 7λ [25], and even in this case, the computational time reaches values of a couple of weeks [25].

There are situations, however, when it is necessary to characterize optical properties of significantly larger-scale material systems, for instance, dielectric interfaces or large-scale optically inhomogeneous media. These properties may include reflectivity, transmittivity, and diffuse scattering properties. One possible way to approach this modeling problem is to consider using a finite-width Gaussian beam as the excitation field instead of a plane wave [10]. However, in this case the result will be corrupted by the undesirable multiple reflections on the boundaries of the computational do-

main, which complicate significantly the interpretation of the calculated scattered field especially for oblique angles of incidence [10]. These multiple reflections can be eliminated by using some analog of absorbing boundary conditions [26] or a perfectly matched layer (PML) [27,28], which are in common use in FDTD and finite-element method calculations. However, in application to the CDA and in our particular situation the use of a PML has several disadvantages. First, the CDA is usually formulated for nonmagnetic materials, but the ideal PML needs nonunitary permeability. Second, in the FDTD and FEM techniques, the PML eliminates scattering from artificial boundaries outside the scatterer in free space. However, in the coupled dipole method only the volume of the scatterer is discretized. That means the PML should match the boundary of the scatterer, which is not a trivial problem for the case of an inhomogeneous material.

We will discuss now another possible way of using the CDA to describe the electromagnetic interaction with large-size, optically inhomogeneous, materials. A slab of inhomogeneous material can be described by replicating the modeling cube in two dimensions; the periodicity in the xy plane is specified by the dimensions of the modeling cube d.

Let us consider the situation where a plane wave

$$\mathbf{E}^{\mathrm{inc}}(\mathbf{r}_j) = \mathbf{E}_0^{\mathrm{inc}} \exp(i\mathbf{k}\cdot\mathbf{r}_j) \tag{4}$$

is incident onto the slab of our quasi-inhomogeneous material at some arbitrary angle. According to the periodicity condition for this type of excitation, the following relation should be satisfied for the field inside the slab:

$$\mathbf{E}(\mathbf{r}_j + nd\hat{\mathbf{x}} + md\hat{\mathbf{y}}) = \mathbf{E}(\mathbf{r}_j)\exp[i\mathbf{k}^{\parallel}\cdot(nd\hat{\mathbf{x}} + md\hat{\mathbf{y}})]. \tag{5}$$

Here $\hat{\mathbf{x}}$ and $\hat{\mathbf{y}}$ are unit vectors in the x and y directions in the plane of the surface of the slab and $\mathbf{k}^{\parallel}$ is the component of the incident wave vector parallel to the surface of the slab; the structural periodicity d is the same along both x and y directions. Using the periodicity relation (5), the master equation for the coupled dipole approximation, i.e., Eq. (1), can now be rewritten as

$$\mathbf{E}(\mathbf{r}_j) = \mathbf{E}^{\mathrm{inc}}(\mathbf{r}_j) + \sum_{\mathbf{r}_k\in V_d}^{N} \alpha_k A_m(\boldsymbol{\rho}_{jk}, |z_j - z_k|)\mathbf{E}(\mathbf{r}_k), \tag{6}$$

where

$$A_m(\boldsymbol{\rho}_{jk}, |z_j - z_k|) = \sum_{m,n=-\infty}^{\infty} A(\mathbf{r}_j, \mathbf{r}_k + nd\hat{\mathbf{x}} + md\hat{\mathbf{y}}) \times \exp[i\mathbf{k}^{\parallel}\cdot(nd\hat{\mathbf{x}} + md\hat{\mathbf{y}})] \tag{7}$$

is the modified Green's function and $\boldsymbol{\rho}_{ij}$ is the projection of vector $(\mathbf{r}_i - \mathbf{r}_j)$ onto the xy plane. The summation in Eq. (6) is performed over all the dipoles in the modeling cube. The summation in the expression for the Green's function (7) is performed over the entire layer of dipoles arranged in a square lattice with constant d. Unfortunately, the lattice sums in Eq. (7) do not converge in real space and special techniques are required to enforce their convergence.

When calculating the lattice sums, we should distinguish between two different situations. First, when $(z_j - z_k) \neq 0$, referring to the interaction between dipoles situated in different planes, the lattice sums may be calculated after applying a two-dimensional Fourier transformation (Ewald's threefold integral transform) [29]. After performing the Fourier transformations one can obtain the following expressions for the lattice sums in the form of a decomposition into propagating and evanescent harmonics [29]:

$$A_m^f(\mathbf{k}^{\parallel}, |z_j - z_k|) = \frac{i2\pi}{d^2} \sum_{p,q=-\infty}^{\infty} \frac{\mathbf{k}_{pq} \otimes \mathbf{k}_{pq} - k^2 I_3}{\kappa_{pq}} \times \exp(i\kappa_{pq}|z_j - z_k|)\exp(i\mathbf{k}_{pq}\cdot\boldsymbol{\rho}_{jk}). \tag{8}$$

Here the superscript f denotes that the expression for the Green's function is written for Fourier space, and

$$\mathbf{k}_{pq} = [\mathbf{k}^{\parallel} + \mathbf{g}_{pq}^{\parallel}, \mathrm{sgn}(z_j - z_k)\kappa_{pq}], \quad \mathbf{g}_{pq}^{\parallel} = \frac{2\pi}{d}(p\hat{\mathbf{x}} + q\hat{\mathbf{y}}),$$

$$\kappa_{pq} = \sqrt{k^2 - (\mathbf{k}^{\parallel} + \mathbf{g}_{pq}^{\parallel})^2},$$

where p and q are integers.

In the second case, when $(z_j - z_k) = 0$, referring to dipole interaction within the same plane, the sum does not converge in real space and it diverges in Fourier space, so another strategy is necessary. In Ref. [30], a method is suggested based on a onefold Ewald transform that provides a rapid convergence for these types of sum. However, this method works correctly only for $d \ll \lambda$, while in our practical situation we are interested in relaxing this strict restriction on d.

One possible way to calculate the sum in Eq. (7) for the case $(z_j - z_k) = 0$ is to write it as a combination of sums in both real and reciprocal spaces [16]:

$$A_m(\boldsymbol{\rho}_{jk}, 0) = A_m^f(\mathbf{k}^{\parallel}, h) + [A_m(\boldsymbol{\rho}_{jk}, 0) - A_m(\boldsymbol{\rho}_{jk}, h)]. \tag{9}$$

The sum in real space, $A_m(\boldsymbol{\rho}_{jk}, h)$, and the one in reciprocal space, $A_m^f(\mathbf{k}^{\parallel}, h)$, are the same as those in Eqs. (7) and (8), but now the distance between the observation point and the lattice of dipoles $|z_j - z_k|$ is replaced by an offset parameter h. The value of this offset parameter h should be chosen to ensure the fastest convergence of the lattice sums.

Using the expressions in Eqs. (7)–(9), one can now evaluate all the summations involved in Eq. (6). The coupled dipole interaction can therefore be calculated for a slab of random material without having to account for the influence of side boundaries.

V. APPLICATION OF THE FAST FOURIER TRANSFORM TO THE MODIFIED CDA FORMALISM

There is still another technical aspect of this modeling approach. The expression for the Green's function in Eq. (7) is no longer a function of the separation vector between two different points on the lattice, but depends on the position of the observation point. As was mentioned, the coupled dipole approximation involves solving a large and dense system of equations, and it is often necessary to use specialized numerical techniques that may drastically improve the efficiency of reaching a solution. The most common technique is the use of a Fourier transform and an iterative approach to the solution such as the conjugate gradient algorithm. This

technique requires the transformed function to be dependent only on the separation between two points, and so the Green's function introduced above should be rewritten to satisfy this condition.

The problem can be solved by writing the master CDA interaction equation not in terms of the actual fields, but using instead fields for which the spatial variation of the phase has been suppressed. This is accomplished by multiplying both sides of Eq. (6) by $\exp(-i\mathbf{k}^{\parallel}\cdot\mathbf{r}_j)$, to obtain

$$\mathbf{E}(\mathbf{r}_j)e^{-i\mathbf{k}^{\parallel}\cdot\mathbf{r}_j}=\mathbf{E}_0^{\mathrm{inc}}(\mathbf{r}_j)e^{-i\mathbf{k}^{\parallel}\cdot\mathbf{r}_j}+\sum_{\mathbf{r}_k\in V_d}^{N}A_{sm}(r_{jk})\alpha_k[\mathbf{E}(\mathbf{r}_k)e^{-i\mathbf{k}^{\parallel}\cdot\mathbf{r}_k}]. \tag{10}$$

Here

$$A_{sm}(|\boldsymbol{\rho}_{jk}|,|z_j-z_k|)=A_m(\boldsymbol{\rho}_{jk},|z_j-z_k|)\exp(-i\mathbf{k}^{\parallel}\cdot\boldsymbol{\rho}_{jk}) \tag{11}$$

is the modified Green's function which depends only on the separation vector. The system of equations (10) can then be solved for the new fields whose phases no longer depend on the spatial coordinates. After a solution is found using the procedure outlined in the preceding section, the actual values of the field are determined by adding the necessary spatially varying phase to the calculated fields.

VI. AN ANALYTICAL SOLUTION TO THE SCATTERING PROBLEM

We will show now that there is a situation where an analytical expression for lattice sums can be found. That is, based on the principle of conservation of energy, the imaginary part of the lattice sum in Eq. (7) can be evaluated analytically.

Let us consider a monolayer of dipoles with a polarizability α arranged in a square lattice. Using the symmetrization procedure described before, the amplitude of the electric field vector at the location of any dipole on the lattice may be written as

$$\mathbf{E}_0=[I_3-\alpha A_{sm}(0,0)]^{-1}\mathbf{E}_0^{\mathrm{inc}}. \tag{12}$$

Using Eq. (10), the expressions for the reflected and transmitted waves in the wave zone can be calculated to be

$$\mathbf{E}_R=\sum_{pq}\mathbf{E}_R^{pq}=-\frac{2\pi i\alpha}{d^2}\sum_{p,q}\frac{\mathbf{k}_{pq}^{+}\times(\mathbf{k}_{pq}^{+}\times\mathbf{E}_0)}{\kappa_{pq}}\exp(i\mathbf{k}_{pq}^{+}\cdot\mathbf{r}),$$

$$\mathbf{E}_T=\mathbf{E}_0^{\mathrm{inc}}+\sum_{pq}\mathbf{E}_T^{pq}=\mathbf{E}_0^{\mathrm{inc}}-\frac{2\pi i\alpha}{d^2}\sum_{p,q}\frac{\mathbf{k}_{pq}^{-}\times(\mathbf{k}_{pq}^{-}\times\mathbf{E}_0)}{\kappa_{pq}}\exp(i\mathbf{k}_{pq}^{-}\cdot\mathbf{r}), \tag{13}$$

where the summation is performed over p,q for which κ_{pq} is real; $\mathbf{k}_{pq}^{\pm}=(\mathbf{k}^{\parallel}+\mathbf{g}_{pq}^{\parallel},\pm\kappa_{pq})$. Let us further assume that the dipole polarizability α is real (absorption-free). In this case the energy conservation law should be satisfied, and the incoming and outgoing fluxes through the planes parallel to the plane of the dipoles should be equal:

$$|\mathbf{E}_0^{\mathrm{inc}}|^2\frac{\kappa_{00}}{k}=\sum_{pq}|\mathbf{E}_R^{pq}|^2\frac{\kappa_{pq}}{k}+{\sum_{pq}}'|\mathbf{E}_T^{pq}|^2\frac{\kappa_{pq}}{k}+\left|\mathbf{E}_0^{\mathrm{inc}}-\frac{2\pi i\alpha}{\kappa_{00}d^2}\times[\mathbf{k}\times(\mathbf{k}\times\mathbf{E})]\right|^2\frac{\kappa_{00}}{k}. \tag{14}$$

The prime on the second sum means that the summation does not include the term $p=q=0$. In obtaining this expression, it was taken into account that the cosine of the angle between the wave vector of the pq outgoing wave and normal to the surface equals κ_{pq}/k. Substituting the expressions (13) into Eq. (14) results in the following relation:

$$\frac{\pi\alpha k}{d^2}\sum_{pq}\frac{k}{\kappa_{pq}}[2k^2|\mathbf{E}_0|^2-|(\mathbf{k}_{pq}^{+}\mathbf{E}_0)|^2-|(\mathbf{k}_{pq}^{-}\cdot\mathbf{E}_0)|^2]+\mathbf{E}_0^{\mathrm{inc}}\cdot[\mathbf{k}\times(\mathbf{k}\times\mathrm{Im}\,\mathbf{E}_0)]=0. \tag{15}$$

After substituting Eq. (12) in Eq. (15), we should demand that all the coefficients in front of $(\mathbf{E}_0^{\mathrm{inc}})_\mu(\mathbf{E}_0^{\mathrm{inc}})_\nu$ $(\mu,\nu=x,y,z)$ be equal to 0. Having satisfied all these conditions, one finds that

$$\mathrm{Im}(A_{sm}(0,0))_{\mu\nu}=\frac{2\pi}{d^2}\sum_{pq}\frac{k^2\delta_{\mu\nu}-(\mathbf{k}_{pq})_\mu(\mathbf{k}_{pq})_\nu}{\kappa_{pq}}, \tag{16}$$

$$(A_{sm}(0,0))_{xz}=(A_{sm}(0,0))_{yz}=0.$$

Note that, if one tries to calculate the lattice sums (7) directly, then it will appear that the expression (16) is not satisfied. This apparent contradiction is resolved by taking into account the dipole self-interaction (radiation friction) [31,32]. After adding the term $i\frac{2}{3}k^3\delta_{\mu\nu}$ to the right-hand side of Eq. (7), the equality (16) will be satisfied exactly. Taking this into account, the expression for the imaginary part of the lattice sums (7) may be written as

$$\mathrm{Im}(A_m(0,0))_{\mu\nu}=\frac{2\pi}{d^2}\sum_{pq}\frac{k^2\delta_{\mu\nu}-(\mathbf{k}_{pq})_\mu(\mathbf{k}_{pq})_\nu}{\kappa_{pq}}-\frac{2}{3}k^3\delta_{\mu\nu},$$

$$(A_m(0,0))_{xz}=(A_m(0,0))_{yz}=0. \tag{17}$$

With this analytical expression for the imaginary part of the interaction, an efficient convergence algorithm can be written to assess the limits of the internal summations and aid in determining an effective value for the offset parameter h.

We should note that usually the basic equations of the CDA (1) are written without the self-interaction term. Instead of introducing an additional term into the equations, the authors take into account self-interaction through the correction to the polarizability [33].

VII. NUMERICAL TESTS

We first tested situations where the material is homogeneous. In this case, analytical solutions for the field inside the slab as well as the corresponding reflection coefficients can be easily found using Fresnel formulas [34]. Figure 2 compares the field distribution inside a slab calculated analytically using the Fresnel formulas and the field calculated

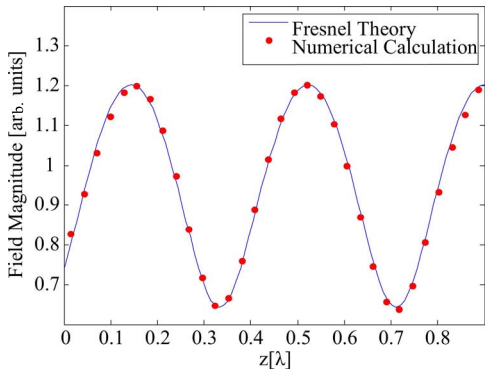

FIG. 2. (Color online) Electric field magnitude inside a plane-parallel slab with refractive index 1.5 (32 dipoles for a thickness of 0.9λ); angle of incidence is 45°. The continuous curve represents the analytical prediction, while the dots denote the results obtained using the CDA extension to infinite media.

numerically using our CDA approach. The results demonstrate the excellent agreement between the two estimates.

Next, the numerical procedure was applied to a slab of inhomogeneous material consisting of small spherical inclusions embedded into a dielectric host. The size of the modeling cube was 0.9λ, and the inclusions were randomly distributed in proportions according to the sample's composition. To describe one realization of an inhomogeneous material, a standard MATLAB random-number generator was used to assign sequentially three-dimensional (3D) coordinates to each inclusion, taking care to ensure that particles did not overlap. Once an inclusion center location was chosen at random, all possible interfering centers were removed from possible selection until the desired volume fraction was reached or all center locations were exhausted. A large number of realizations (100) of a sample were generated and the amplitude of the reflected wave was calculated for every realization.

Figure 3 presents the average value and the standard deviation of the reflection coefficient calculated from the obtained ensemble of reflected wave amplitudes. The reflection coefficients were calculated for different concentrations and for different dimensions of inclusions. To model spherical inclusions on the cubic lattice, spheres consisting of one (equivalent radius 0.017λ), seven (equivalent radius 0.033λ), and 33 dipoles (equivalent radius 0.056λ) were considered. The numerical results were compared with estimations of an effective medium description of the material's properties. The refractive index of this effective medium was calculated based on the Bruggeman formalism [35]:

$$(1-f)\frac{n_h^2-n_{\text{eff}}^2}{n_h^2+2n_{\text{eff}}^2}+f\frac{n_i^2-n_{\text{eff}}^2}{n_i^2+2n_{\text{eff}}^2}=0, \tag{18}$$

where f is the volume fraction of inclusions, n_h, n_i are the refractive indices of the host and inclusion, respectively, and n_{eff} is the effective refractive index. The coefficients of reflection were then found using Fresnel's formula. In this specific situation all the relevant length scales (dimensions of the inclusions and the distances between inclusions) were much smaller than the wavelength, and the Bruggeman formalism should provide a good description of the optical properties. As can be seen in Fig. 3, this is confirmed by the good agreement between the results of the numerical simulation and the effective medium predictions. However, one can also notice that the increase in the size of the inclusions leads to an increase of the standard deviation of the reflected intensity. The standard deviation reaches a maximum value at some specific volume fraction (about 10%) that corresponds to a situation where there is a large inclusion contribution to the scattered intensity simultaneously with significant variability in the position of inclusions. Of course, these variations between different realizations of the random medium cannot be described within the framework of effective medium theory. One could also expect deviations of the numerical results from the Bruggeman description for large concentrations of inclusions because of multipolar interactions. The possible reason why we do not observe it in Fig. 3 for concentrations close to 50% is that the reflectivity is relatively high in this region, and should not depend much on the effective refractive index change.

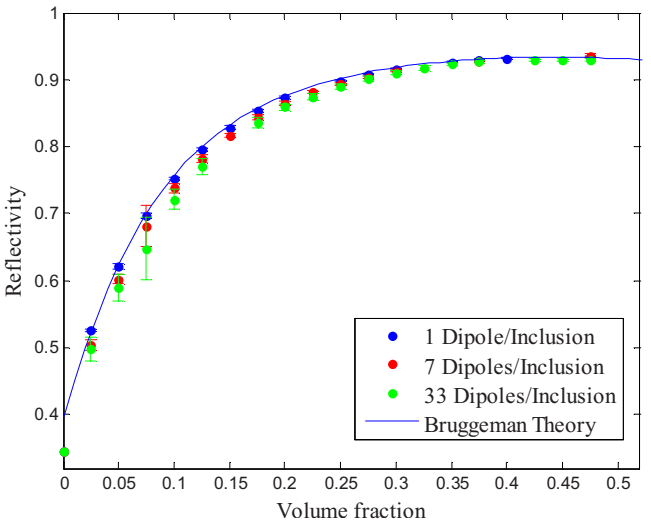

FIG. 3. (Color online) Amplitude reflection coefficient as a function of volume fraction of inclusions. The solid line represents the analytical prediction of the Bruggeman model combined with the Fresnel theory, while the dots denote the results of CDA simulations for different sizes of inclusions. The bars indicate the standard deviation in the distribution of reflected wave amplitude for different realizations of the random medium. Parameters of the calculation: the thickness of the slab is 0.9 wavelength, modeling cube is represented by $32\times32\times32$ dipoles, refractive index of the host is $n_h=1.5$, refractive index of inclusions is $n_i=2$, and the angle of incidence is 75°.

VIII. FURTHER DISCUSSION AND CONCLUSIONS

One feature that has not been discussed thus far is the influence of the periodicity on the scattered fields. In general, the scattering of a plane wave from a periodic structure results in diffracted orders that depend on the wavelength and the periodicity length [34]. Increasing the periodicity parameter, one increases the number of diffractive orders. This is illustrated in Fig. 4 where the directions of the diffracted

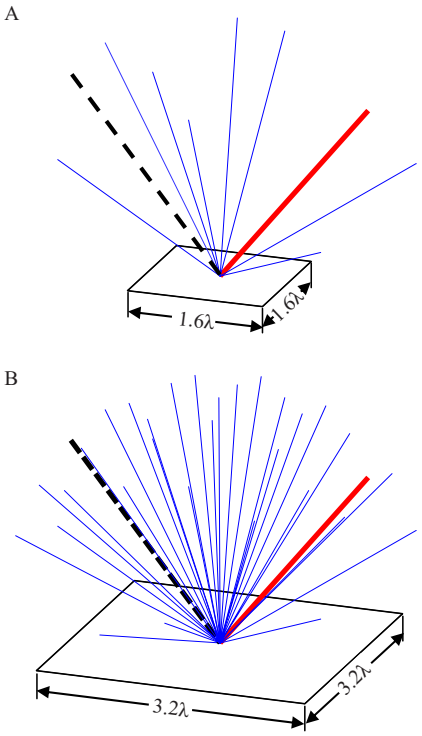

FIG. 4. (Color online) Directions of diffractive orders for periodicity parameter equal to (A) 1.6λ and (B) 3.2λ. The dashed line denotes the direction of the **k** vector of the incident wave; the thick line shows the direction of specular reflected light (zero-order diffraction).

orders are shown for different periodicity parameters and in the case of a plane-wave incident field at 45°.

It is possible to show that, in the case of a homogeneous material, only the zero-order diffraction is present, irrespective of the periodicity parameter d; this order corresponds to the specularly reflected wave. In the case of an inhomogeneous material, on the other hand, additional diffractive orders appear, carrying the energy corresponding to the scattered field. The presence of additional diffraction orders was mentioned also in Ref. [36], where the light scattering in an absorbing medium with randomly distributed scatterers was modeled in 2D geometry. However, in Ref. [36], the authors consider these diffractive orders as a side effect of the method, arising because of the constraint imposed on particle arrangement within the modeling cell. According to the method presented in Ref. [36], no particle center could be at a distance smaller than the radius from the edge of the cell. This limitation is absent in the CDA where inclusions may wrap around the boundaries. The meaning of discrete diffractive orders in the case of the CDA can be understood by this simple argument. Let us suppose that the periodicity approaches infinity; then the directions of the diffractive orders occupy the entire space, which reproduces the diffuse light scattered by the inhomogeneous material. Thus, these additional diffractive orders that appear in the simulations serve as measures of diffuse light: the larger the periodicity parameter we use in the CDA simulations, the more precisely we can describe the properties of diffusely scattered light. The ensemble of discrete orders in the CDA result represents the sampled version of the field scattered by an infinitely extended random medium. The properties of this diffuse light in CDA simulations will be discussed in more detail in future presentations.

In conclusion, we introduced an extension of the coupled dipole method for dealing with slabs of inhomogeneous materials. We demonstrated that this method can adequately describe optical properties such as specular and diffuse reflection amplitudes. The accuracy of our approach was tested on slabs with thicknesses less than the wavelength of light. We found an excellent agreement with analytical results for slabs of homogeneous media and for media containing small-size inclusions. When the size of the inhomogeneities increases, our numerical approach can describe phenomena for which no analytical models are available.

In future reports we will illustrate the use of this method for describing statistical aspects of the optical properties of inhomogeneous slabs. This will require increasing the periodicity parameter d to dimensions larger than the wavelength.

A possible generalization of our model is the description of semi-infinite inhomogeneous medium. However, in this case the direct application of our approach is not possible, because the electromagnetic field in the z direction is not exactly periodic. The presence of the surface breaks the symmetry and makes the field close to the surface different from that in the bulk. The generalization procedure should take this into account.

Another particular direction of interest is modeling roughness effects by introducing irregularities into the upper surface of the modeling layer. In the case of the coupled dipole method, media with irregular surface structure represent a particular case of inhomogeneities where some surface dipoles have zero polarizability. Thus, the formalism described here for inhomogeneous media is valid also for media with rough surfaces. Finally, we would like to note that the approach introduced in this paper may, in principle, be extended to the case of illumination with nonuniform beams by applying a plane-wave decomposition of the incident fields.

ACKNOWLEDGMENTS

This research was partially supported by the Army Research Office.

[1] G. Zaccanti, Appl. Opt. **30**, 2031 (1991).
[2] A. Ishimaru, *Wave Propagation and Scattering in Random Media* (Academic Press, New York, 1978).
[3] V. L. Kuz'min and V. P. Romanov, Phys. Usp. **39**, 231 (1996).
[4] M. C. W. van Rossum and T. M. Nieuwenhuizen, Rev. Mod. Phys. **71**, 313 (1999).
[5] L. Tsang and J. A. Kong, *Scattering of Electromagnetic Waves: Advanced Topics* (Wiley, New York, 2001).
[6] *Waves and Imaging through Complex Media*, edited by P. Sebbah (Springer, Berlin, 2001).
[7] M. I. Mishchenko, L. D. Travis, and A. A. Lacis, *Multiple Scattering of Light by Particles: Radiative Transfer and Coherent Backscattering* (Cambridge University Press, Cambridge, U.K., 2006).
[8] S. H. Tseng, A. Taflove, D. Maitland, and V. Backman, Radio Sci. **41**, RS4009 (2006).
[9] M. I. Mishchenko, Li Liu, D. W. Mackowski, B. Cairns, and G. Videen, Opt. Express **15**, 2822 (2007).
[10] C. Meiners and A. F. Jacob, Electromagnetics **26**, 235 (2006).
[11] E. M. Purcell and C. R. Pennypacker, Astrophys. J. **186**, 705 (1973).
[12] B. T. Draine and P. J. Flatau, J. Opt. Soc. Am. A **11**, 1491 (1994).
[13] R. Schmehl, B. M. Nebeker, and E. D. Hirleman, J. Opt. Soc. Am. A **14**, 3026 (1997).
[14] P. C. Chaumet and M. Nieto-Vesperinas, Phys. Rev. B **61**, 14119 (2000); **62**, 11185 (2000); **64**, 035422 (2001).
[15] A. Rahmani, P. C. Chaumet, and F. de Fornel, Phys. Rev. A **63**, 023819 (2001).
[16] P. C. Chaumet, A. Rahmani, and G. W. Bryant, Phys. Rev. B **67**, 165404 (2003).
[17] P. C. Chaumet and A. Sentenac, Phys. Rev. B **72**, 205437 (2005).
[18] A. Penttilä, K. Lumme, and L. Kuutti, Appl. Opt. **45**, 3501 (2006).
[19] A. Lakhtakia, Astrophys. J. **394**, 494 (1992).
[20] P. J. Flatau, Opt. Lett. **22**, 1205 (1997).
[21] R. Barrett, M. Berry, T. F. Chan, J. Demmel, J. Donato, J. Dongarra, V. Eijkhout, R. Pozo, C. Romine, and H. Van der Vorst, *Templates for the Solution of Linear Systems: Building Blocks for Iterative Methods* (SIAM, Philadelphia, PA, 1994).
[22] J. J. Goodman, B. Draine, and P. J. Flatau, Opt. Lett. **16**, 1198 (1991).
[23] A. Apostol, D. Haefner, and A. Dogariu, Phys. Rev. E **74**, 066603 (2006).
[24] M. Rusek and A. Orłowski, Phys. Rev. E **56**, 6090 (1997).
[25] M. A. Yurkin, V. P. Maltsev, and A. G. Hoekstra, J. Quant. Spectrosc. Radiat. Transf. **106**, 546 (2007).
[26] G. Mur, IEEE Trans. Electromagn. Compat. **EMC-23**, 377 (1981).
[27] M. Kuzuoglu and R. Mittra, IEEE Microw. Guid. Wave Lett. **6**, 447 (1996).
[28] Z. S. Sacks, D. M. Kingsland, R. Lee, and J.-F. Lee, IEEE Trans. Antennas Propag. **43**, 1460 (1995).
[29] C. M. J. Wijers and G. P. M. Poppe, Phys. Rev. B **46**, 7605 (1992).
[30] G. P. M. Poppe, C. M. J. Wijers, and A. van Silfhout, Phys. Rev. B **44**, 7917 (1991).
[31] A. V. Ghiner and G. I. Surdutovich, Phys. Rev. E **56**, 6123 (1997).
[32] V. A. Alekseev, A. V. Vinogradov, and I. I. Sobelman, Sov. Phys. Usp. **102**, 43 (1970).
[33] TheB. T. Draine, Astrophys. J. **333**, 848 (1988).
[34] M. Born and E. Wolf, *Principles of Optics* (Cambridge University Press, Cambridge, U.K., 1999).
[35] D. A. G. Bruggeman, Ann. Phys. (Leipzig) **24**, 636 (1935).
[36] S. Durant, O. Calvo-Perez, N. Vukadinovic, and J.-J. Greffet, J. Opt. Soc. Am. A **24**, 2953 (2007).